Earth and Planetary Science Letters 310 (2011) 286–292

Contents lists available at SciVerse ScienceDirect

Earth and Planetary Science Letters

journal homepage: www.elsevier.com/locate/epsl

Interaction between pyroclastic density currents and buildings: Numerical simulation and first experiments

Domenico M. Doronzo, Pierfrancesco Dellino *

Centro Interdipartimentale di Ricerca sul Rischio Sismico e Vulcanico (CIRISIVU)-c/o Dipartimento di Scienze della Terra e Geoambientali, Università degli Studi di Bari, Bari, Italy

ARTICLE INFO

Article history:
Received 21 December 2010
Received in revised form 19 July 2011
Accepted 11 August 2011
Available online 29 September 2011

Editor: L. Stixrude

Keywords:
pyroclastic density current
flow–building interaction
simulation
experiment

ABSTRACT

The interaction between pyroclastic density currents and buildings is investigated by means of numerical simulation and large-scale experiments. Numerical simulation is performed with the Euler–Lagrange approach using a two-way coupling between gas and particles of three sizes. The collapse of an eruptive column consisting of a mixture of gas and pyroclasts is produced experimentally, and the impact of the resulting shear current with mock-ups representing buildings is monitored. A combination of results from simulations and experiments shows that, upon impact with a building, the multiphase current develops strong turbulence intensity, which significantly affects particle dispersion. The flow recirculation around the building induces forced deposition at the front and wake in the back wall, with flow reattachment farther away. These changes produce a variation in the dynamic pressure, which is the most important parameter for assessing the impact of pyroclastic density currents moving over inhabited areas.

1. Introduction

Pyroclastic density currents (PDCs) are ground hugging gas–particle (pyroclasts) flows that move at high velocity down the volcano and over the surrounding terrain (Cas and Wright, 1987). They can be generated by the collapse of an eruptive column (e.g. Dellino et al., 2010a) or by lava–dome collapse (Esposti Ongaro et al., 2008).

PDCs can range over a wide spectrum of particle volumetric concentration, and have a fluid-dynamic behavior spanning dispersed to dense flow (Crowe, 2006). Dilute PDCs, which represent the dispersed end member, behave as turbulent wall flows (Pope, 2000), resembling the boundary layers (TBLSF) (Dellino et al., 2008) of fluid dynamics (Cebeci and Cousteix, 1999; Schlichting and Gersten, 2000).

PDCs are very dangerous because they can move at high velocity for several kilometers (Cas and Wright, 1987) and, upon reaching inhabited areas, they impact buildings at high dynamic pressure $P_{dyn} = 0.5\rho_f u^2$ (Valentine, 1998), where ρ_f is the gas–particle mixture density and u is flow velocity. Because of the strong flow stratification, the impact is stronger in the lower part of the current (Dellino et al., 2008; Valentine, 1987). Generally, the areas of extensive PDC–building interaction, such as villages and cities, are located several kilometers from the volcanic vent. It is therefore likely that PDCs that originated both as relatively dispersed and dense currents reach inhabited areas as dilute currents (Doronzo, 2010), because of previous particle deposition, atmospheric air entrainment and interaction with topography (Doronzo et al., 2010; Giordano, 1998). This is the situation investigated in this paper, where the interaction between a PDC and a building is numerically simulated, and results are compared with experiments. The flow-field variables are analyzed both before and upon impact with the building. These aspects have never been thoroughly investigated in previous numerical simulation of PDCs, since they lack detail at the base of the current, and also lack the presence of buildings.

2. Numerical analysis of PDC–building interaction

The concepts behind the numerical approach, and the various steps of simulation, are summarized here. A detailed discussion of the model equations is found in Doronzo et al. (2010) and briefly reported in the Supplementary material.

An Euler–Lagrange numerical scheme is adopted for simulating the multiphase behavior of PDCs (Doronzo et al., 2011). It consists of treating the gas phase as a continuum and the pyroclasts as a discrete phase. Such an approach can be applied to multiphase mixtures having no more than 12% particle volumetric concentration (Bakker, 2008), which is guaranteed in our case, since the current reaches the building in relatively dilute conditions (as discussed in Section 1).

A 2D unsteady, compressible RANS (Reynolds Averaged Navier–Stokes) simulation of PDCs is performed on a computational domain 200 m long and 50 m high, which contains a 10 m × 10 m building located at 80 m from the inflow. The grid (Fig. 1) is of a non-uniform

* Corresponding author.
E-mail address: dellino@geomin.uniba.it (P. Dellino).

0012-821X/$ – see front matter © 2011 Elsevier B.V. All rights reserved.
doi:10.1016/j.epsl.2011.08.017

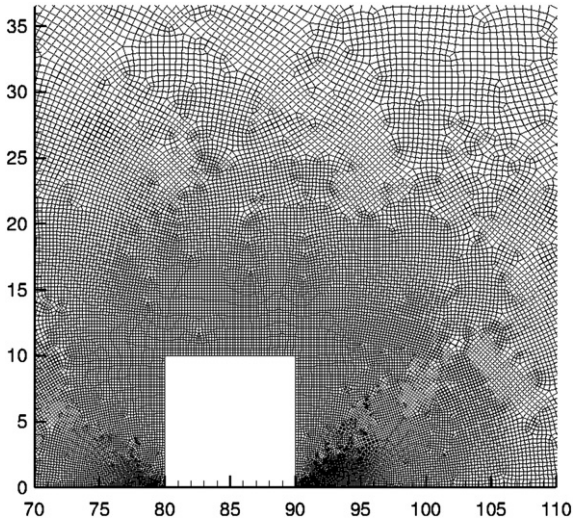

Fig. 1. Detail of the mesh used for the numerical simulation. The mesh is highly refined at the bottom surface and along the building walls, in order to allow a detailed reconstruction of the strong gradients near solid surfaces.

unstructured type, and has 40,958 quadrilateral cells with an individual area ranging from 4 cm^2 (base) to 100 cm^2 (top).

The set of equations for the gas phase, which is a multispecies mixture of volcanic gas and atmospheric air, is defined by the conservation equations for mass, momentum, energy and gas species, and it can be referred to a classic computational fluid-dynamics problem of convection–diffusion dominated flows (Fletcher, 1991). Turbulence is modeled with a two-equation model, the realizable k–ε one of Shih et al. (1995) that solves for the unknown turbulent viscosity by accounting for the mean deformation and rotation rates, which we expect to be high where flow separation and recirculation occur (Blocken and Carmeliet, 2007; Defraeye et al., 2010), i.e. around the building (Doronzo, 2010). The turbulence model is coupled with non-equilibrium wall functions to account for the presence of the building. In particular, the one for momentum is sensitive to the effects of pressure gradients, and departure from equilibrium, in the zones where the mean flow and turbulence change rapidly. The role of the wall functions is that of bridging the very near-wall flow region (viscous sublayer and buffer layer), which is affected by molecular viscosity, with the fully turbulent region, without directly using the k–ε model near the wall (Pope, 2000; Schlichting and Gersten, 2000).

The dynamics of the solid phase are defined by the equation of Lagrangian particle motion, which solves for particle trajectories on the basis of the fluid solution. The solid phase consists of three sizes of pyroclasts (2.8 mm, 1.4 mm and 0.064 mm), which represent the dominant range between ash and lapilli that is expected to be transported by turbulent suspension in a PDC. A stochastic tracking model, which is based on the assumption of isotropic turbulence, is used to account for the effects of the fluctuating fluid solution on the particles, the so-called turbulent dispersion, which we expect to be strong around the building. Particles are two-way coupled with gas, which means that they are transported by the gas (one-way), and at the same time they can influence fluid turbulence (two-way) (Balachandar and Eaton, 2010; Crowe, 2000). This condition is allowed because in some natural multiphase systems, such as volcaniclastic turbidity currents (Doronzo and Dellino, 2010) and PDCs (Dellino et al., 2007), particles are effective in modulating fluid turbulence (Pope, 2000), and turbulence intensity (ratio of isotropic turbulent kinetic energy to squared reference velocity) can be greatly increased.

The set of equations is solved using Ansys Fluent software (Fluent, 2006), with an implicit, segregated, cell-centered finite-volume technique (Versteeg and Malalasekera, 2007), which means that, for a given dependent variable, the unknown value is computed at each cell center by interpolating the same unknown from the adjacent cell centers. In this way, each variable appears in more than one equation (one/cell) at each time level, so the equations are solved separately for each variable (segregated) but simultaneously (implicit) for all the cells. An iterative method is needed to solve implicitly the system of equations (Versteeg and Malalasekera, 2007), which consists of guessing a solution for an independent variable and solving for the value of the associated dependent variable, while keeping the other dependent variables fixed. The iterative cycle is able to improve the guessed solution, by giving the best one at the last iteration for each time level, before passing to the next level and restarting the cycle on the improved solution.

The equations are second-order accurate by means of an upwind discretization of the convection terms and a central-differencing scheme of the diffusion terms. The transient terms are discretized by means of a three-time level scheme, i.e. a second-order accurate backward-differencing scheme.

The accuracy of the solution is guaranteed by the second-order discretization of both the spatial and temporal terms. The stability of the solution is ensured by the implicit method, which is unconditionally stable (Ferziger and Peric, 2002) and not limited by stability constraints (Anderson, 1995). The trend of errors for each equation is monitored during calculation, and, in some cases, reduced by means of an under-relaxation technique (Anderson, 1995; Ferziger and Peric, 2002; Patankar, 1980). Convergence of solution is controlled by checking that the residuals, which represent a measure of the errors, decrease to less than 10^{-3} for each equation.

3. Boundary and initial conditions of simulation

In volcanology, it is always critical to set the boundary and initial conditions to be used for simulating PDCs (Dartevelle et al., 2004; Dufek and Bergantz, 2007; Neri et al., 2003; Valentine and Wohletz, 1989). In our case, these conditions are obtained from experimentally validated preliminary models (Dellino et al., 2008, 2010a, 2010b), which we use to calculate the input data for the simulation, such as the time-averaged flow velocity and density profiles. For our simulation, we apply as gas inflow (left vertical side of the domain of Fig. 1) a vertical profile of horizontal velocity, according to the logarithmic law of the wall for rough flows (Furbish, 1997), which is calculated with the geophysical model of Dellino et al. (2008). This calculation is based on the approximation of PDCs to TBLSFs, as described in Section 1. In particular, the inflow input data are those of a PDC that occurred during the AD 472 (Pollena) eruption of Vesuvius (Italy) (Sulpizio et al., 2005), and are calculated at a distance of 4 km from the crater on the basis of the physical features (dimension d, density ρ_s and drag coefficient C_d) of pyroclasts sampled from the natural deposits. In this way, an average particle settling velocity v, is calculated with the model of Dellino et al. (2005), which is equated to the PDC shear velocity u_*, according to the sedimentation criterion of Middleton and Southard (1984)

$$v = \sqrt{\frac{4gd\left(\rho_s - \rho_f\right)}{3C_d\rho_f}} = u_* \tag{1}$$

where

$$\rho_f = \rho_s C + (1-C)\rho_g \tag{2}$$

is the PDC density, C is the pyroclast volumetric concentration, ρ_g is the gas density, which is calculated with a volume-weighted multispecies mixing law, and g is gravity acceleration (9.81 m/s^2).

The time-averaged velocity profile $\overline{u}(y)$ is a function of the flow height y so, given the flow shear velocity from Eq. (1) and a roughness parameter K_s, it follows that

$$\overline{u}(y) = u_* \left[\frac{1}{\kappa} \ln\left(\frac{y}{K_s}\right) + 8.5\right] \quad (3)$$

where κ is the von Karman constant (0.41). The overbar indicates that the velocity u is the time-averaged part of the instantaneous velocity. Eq. (3) is for equilibrium TBLSFs (Pope, 2000), i.e. in absence of obstacles, and the expected departure from this initial condition (as the flow approaches the building) is accounted for by the wall functions (Section 2).

Actually, also ρ_f, through C (Eq. (2)), is a continuous function of y (Rouse, 1939), since PDCs are concentration-stratified flows (Dellino et al., 2008; Valentine, 1987). Here, the pyroclasts enter the domain through six horizontal discrete injections at different inflow heights, each of which is representative of the actual concentration, and velocity, around that height. The concentration gradient is the one calculated by Dellino et al. (2008) for the 4-km (from vent) Pollena eruption (Sulpizio et al., 2005). The spacing between injections decreases downward, in order to better reproduce the steep particle concentration gradient at the base of a PDC (Dellino et al., 2008; Valentine, 1987). The particles, as well as the gas inflow, have an initial temperature of 573 K, which is typical of many PDCs (Branney and Kokelaar, 2002). All PDC input data are given in Table 1.

The outflow (right vertical side and top of Fig. 1) encounters a static pressure of 1 atm as it exits. A no-slip condition is applied along both the bottom surface and the building walls. The whole domain is initialized with a condition of no velocity, turbulence or volcanic gas (static condition for pure atmospheric air). Atmosphere temperature is set to 298 K and static pressure to 1 atm.

Table 1
Input data of the simulated PDC, as calculated from the natural deposits generated by a PDC during the AD 472 eruption of Vesuvius (Italy).

Parameters	Value
Inflow thickness (m)	50
Inflow shear velocity (m/s)	1.88
Inflow velocity at $y=50$ m (m/s)	52.75
Roughness parameter (m)	0.02
Atmospheric air density (kg/m^3)	1.22
Volcanic gas density (kg/m^3)	0.38
Particle density (kg/m^3)	1550
Atmospheric air temperature (K)	298
Volcanic gas temperature (K)	573
Particle temperature (K)	573
Atmospheric air mass fraction (%)	0
Volcanic gas mass fraction (%)	100
Turbulence intensity (%)	5
Turbulence length scale (m)	20.5
Particle drag coefficient	1.72
Particle minimum diameter (m)	0.00006
Particle intermediate diameter (m)	0.0014
Particle maximum diameter (m)	0.0028
Particle velocity at $y=1$ m (m/s)	34.37
Particle velocity at $y=3$ m (m/s)	39.53
Particle velocity at $y=7.5$ m (m/s)	43.84
Particle velocity at $y=15$ m (m/s)	47.09
Particle velocity at $y=25$ m (m/s)	49.49
Particle velocity at $y=40$ m (m/s)	51.70
Particle vol. concentration at $y=1$ m (%)	3.70
Particle vol. concentration at $y=3$ m (%)	1.70
Particle vol. concentration at $y=7.5$ m (%)	0.46
Particle vol. concentration at $y=15$ m (%)	0.23
Particle vol. concentration at $y=25$ m (%)	0.072
Particle vol. concentration at $y=40$ m (%)	0.026
0.00006 m particle vol. concentration (%)	4.56
0.0014 m particle vol. concentration (%)	64.64
0.0028 m particle vol. concentration (%)	30.80

The run works as follows: at the initial instant $t=0^+$, both the volcanic gas and pyroclasts enter the domain, by defining an early multiphase inflow. As the volcanic gas is subject to turbulent entrainment of the surrounding atmospheric air (similarly to what happens in nature) (Hallworth et al., 1993), the pyroclasts rapidly couple to the gas and adapt to the TBLSF before interacting with the building. This happens along the preliminary 80 m between the inlet of the domain and the building. The resulting, computationally-generated PDC, reaches the building as an equilibrated stratified, multiphase TBLSF (Eq. (3)). As the pyroclasts travel along the first 80 m, their trajectories and concentration are adjusted according to gas coupling (Eq. (1)). A similar strategy is adopted in the simulations of wind-driven rain, where droplets adapt to an atmospheric boundary layer (Blocken and Carmeliet, 2006).

The condition of equilibrium is representative of a PDC that travels in a free field, as occurs for natural PDCs, before interacting with inhabited areas. This condition is guaranteed until the PDC approaches the building, which is expected to disturb the flow field towards a non-equilibrium condition (Blocken and Carmeliet, 2007; Defraeye et al., 2010).

4. Experiments

The interaction between a PDC and a building has been reproduced during a dedicated session of large-scale experiments (Dellino et al., 2007, 2010a, 2010b). The experimental setting consists of a volcano-style cone of 13 m base radius and 7° average slope, on which a conduit of 0.3 m radius and variable length from 2.2 m to 3.2 m is centered. Pyroclastic material from Vesuvius is loaded on the base plate of the conduit, and it is expelled as a gas–particle mixture, by means of a controlled injection of pressurized gas, via nozzles carved in the base plate. The gas pressure and material load, as well as the conduit length, are set depending on the eruptive regime to be reproduced (Dellino et al., 2010a). Collapsing columns, overpressured jets and convective plumes can be replicated. Here, we refer to vertical column collapses that generate PDCs. Details of the experimental apparatus and runs can be found in Dellino et al. (2007, 2010a, 2010b).

PDC–building interaction was reproduced in the experiments by means of a cubic mock-up of 0.027 m^3 volume, which was placed over a flank of the cone 5.5 m from the conduit base. In this way, the scenario of a PDC that impacts a building at a certain distance from the volcanic vent is replicated. The distance is chosen so as to allow the condition of a fully developed PDC (Dellino et al., 2007). At that distance, the experimental PDC reaches a Reynolds number greater

Fig. 2. Image showing the experimental current impacting the mock-up.

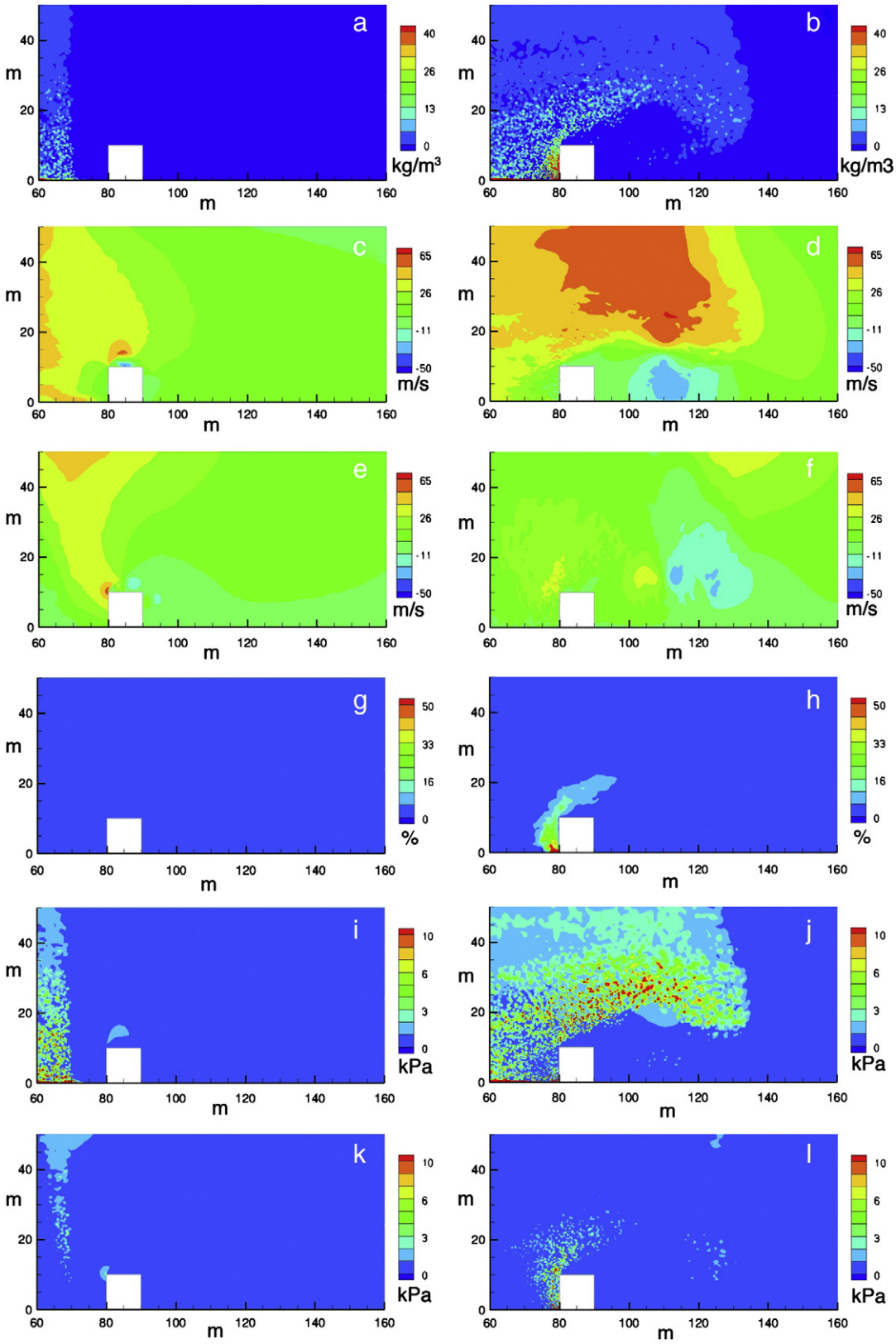

Fig. 3. Montage showing the main flow field variables of the computationally-generated PDC just before (on the left) and upon (on the right) impact with the building. (a) Density due to particles just before impact. (b) Density due to particles upon impact. (c) Horizontal velocity component just before impact. (d) Horizontal velocity component upon impact. (e) Vertical velocity component just before impact. (f) Vertical velocity component upon impact. (g) Turbulence intensity just before impact. (h) Turbulence intensity upon impact. (i) Horizontal component of dynamic pressure just before impact. (j) Horizontal component of dynamic pressure upon impact. (k) Vertical component of dynamic pressure just before impact. (l) Vertical component of dynamic pressure upon impact.

than 10^6 (it is fully turbulent), which does not increase farther away, as it occurs in fully developed TBLSF (Furbish, 1997). In the experiment, the PDC spreads radially over all the cone, and overruns the mock-up (Fig. 2), which roughly behaves as a baffle for the flow. The scaling between simulation and experiments is done by knowing (from previous experiments) the thickness of the experimental PDC, which is about 1.5 m (Dellino et al., 2007, 2010a, 2010b). In order to maintain the same ratio of building and flow thickness (1/5) that is used in the simulation, the height of the mock-up was set to 0.3 m. This ratio, hence both the numerical and experimental results, is scaled to the real case of PDCs propagating over cities composed of buildings about 2 to 5 floors high, such as those in the densely populated area of Vesuvius. If we infer that the largest turbulent eddies have a diameter equal to 0.41 of the total flow thickness (from the mixing-length Prandtl's theory; see Schlichting and Gersten, 2000), and that they transport most of the mechanical energy (Furbish, 1997), then the building is enclosed inside the most energetic turbulent structures, but it is not much smaller than them. This scaling of building to turbulence allows us to investigate how the building, upon impact, influences the turbulent structure of the current.

5. Results and discussion

In the montage of Fig. 3, the main fluid–dynamic variables of the current are shown just before (left) and upon impact with the building (right). This figure shows how the flow–building interaction influences the PDC behavior. The multiphase current compresses air in front of the building even before the PDC reaches the building wall. This causes fluid circulation around the building (Fig. 3c and e) that precedes arrival of the gas–particle mixture (Fig. 3a).

In general, the numerical simulation shows that the particles strongly exchange momentum with the fluid phase, especially where strong gradients of bulk density (Fig. 3b) and velocity (Fig. 3d) occur, i.e. in front, over the roof and behind the building. A strong separation and recirculation of the TBLSF occurs around the building because the equilibrium condition is rapidly lost at the impact, and this is demonstrated by the high values of turbulence intensity shown in Fig. 3h (20–50%) as compared to the very low values before the multiphase current impacts the building (Fig. 3g). The interaction zone around the junction between the ground and the building can be regarded as a concave (destabilizing) surface with infinite curvature (the circle's radius tangent to the junction tends to zero), over which streamlines are strongly curved, and this causes high mixing and turbulence (Hoffmann et al., 1985; Valentine et al., 2011). The horizontal component of fluid velocity in front of the building (Fig. 3d) is a little lower during current passage than just before impact (Fig. 3c), but a vertical velocity component develops around the building (Fig. 3f), which is much higher than what is expected in a unidirectional flow. Particle inertia does not allow the pyroclasts to rapidly readjust to the streamline curvature (Cantero et al., 2008), which would be expected to occur over a convex (stabilizing) surface (Muck et al., 1985; Valentine et al., 2011).

The separation region of the PDC, which mimics the wake region generated around comets (Raga and Cantó, 2008), coincides with the particle wake that envelops the building, as it can be seen by Fig. 3b where the density due to particles is represented. The particles transported in the more concentrated lower part of the PDC, which is not able to flow over the building, are subject to rapid deposition in front of the building and mark a much higher density with respect to the free flow (Fig. 3a). Deposition occurs from the current where it has bulk densities up to 40 kg/m^3 (Fig. 3b). This effect is well replicated by experiments, and in Fig. 4a a detail of particle deposition in front of the mockup is shown, where a thick massive deposit is formed, because of a rapid loss of flow transport capacity. This means that even if the flow is relatively dilute before impacting the building, the deposit formed against the building is quite thick. Particles transported in the more dilute upper part of the PDC, which separates from the lower part, are subject to turbulent dispersion in front of the building. Over the roof, they are involved in a shear layer that has horizontal velocities of about 15 m/s (Fig. 3d). The shear layer reattaches far away from the building, almost at the vertical outlet of the simulation, so the particles are involved in a back flow toward the building. This back flow, consisting of negative horizontal velocities of about 20 m/s (Fig. 3d), represents the lower part of a big recirculation zone, which is generated between the back wall and the reattachment point. Also this characteristic behavior at the flow–building interaction zone is replicated by experiments. In Fig. 4b, a general view of the pyroclastic deposits generated during an experiment (Dellino et al., 2010a, 2010b) is shown, and the distribution of the deposits is consistent with the results of numerical simulation. Around the building, the deposited pyroclasts mark wake regions that start from the obstacle and are elongate in the main flow direction. These regions correspond to shear layers generated during the separation of the PDC. No particles are deposited at the back of the building, as also indicated in the simulation, except for the few ones involved in the recirculation.

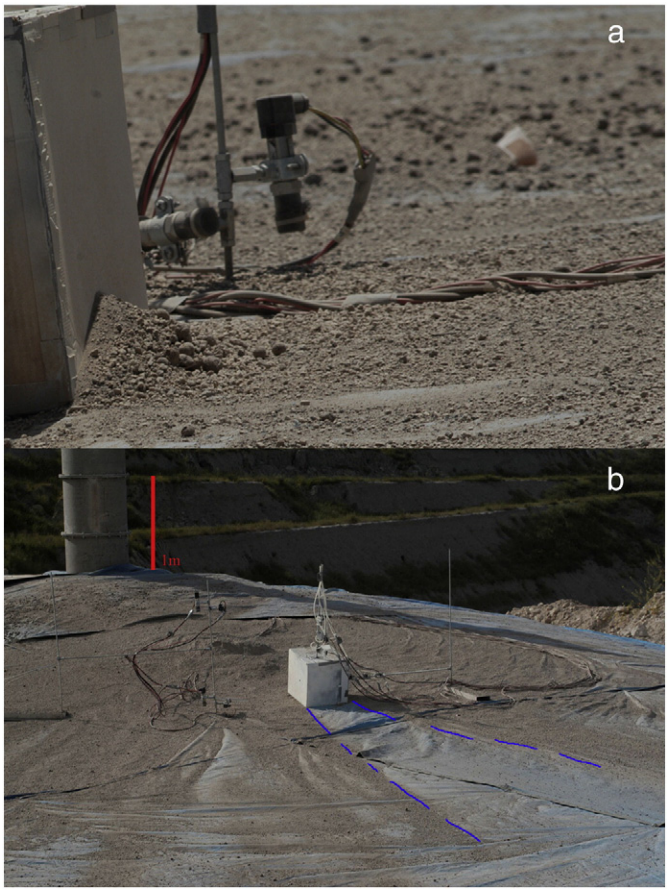

Fig. 4. Photos showing the deposits formed by the passage of an experimental PDC over the mock-up. (a) Detail of the thick massive deposit formed at the front wall. (b) The dashed line shows that in the wake of the current (behind the back wall of the mock-up) particle deposition is highly reduced.

The coupling of gas velocity and particle concentration gives way to drastic changes in the value of dynamic pressure, the distribution of which is very different when comparing the flow before building impact and upon impact. In particular, the horizontal component of dynamic pressure is a little lower upon impact (Fig. 3j), compared to the value for the current before impact (Fig. 3i). Instead, at the front of the building, the vertical component of dynamic pressure is locally very high upon impact (Fig. 3l), which is in contrast negligible in the

current before the impact (Fig. 3k), as is expected in a unidirectional flow.

By matching the results of simulation and experiments, it is possible to extract some general information about the interaction of PDCs with buildings. The impact of a flow at the building front causes a strong disequilibrium in the current, and there is strong recirculation of the flow is realized around the building. The most evident modification of the flow field is therefore the appearance of a strong dispersion effect of the particles around the building. Also the turbulent structure of the current is dramatically changed and particle dispersion causes an abrupt change of turbulence intensity (Fig. 3g vs. 3h), because of particle–gas coupling. This effect clearly changes the large-scale structure of turbulence at the base of the current, which is the most energetic part of the flow. As a result, deposition of coarse particles is greatly enhanced at the building front, whereas finer particles "hydroplane" over the building, since they are included in the wake of the flow, to be reattached to the ground farther away.

6. Concluding remarks on the impacts of PDCs on buildings

By combining data from numerical simulation and experiments, it becomes clear that complex interactions occur when a PDC impacts a building. These effects were not investigated in detail in previous simulations of PDCs because they did not take into consideration the flow–building interaction.

Concerning risk, the main information obtained from this research concerns the great thickening of deposits in front of buildings, the development of a high vertical component of dynamic pressure at the building front, and particle dispersion in the wake of the building. This information is relevant for hazard assessment, since on the upcurrent side a thick deposit (much thicker than the layer that would have formed without the building) would favor burning of flammable materials, since the deposit, because of the low thermal conductivity of its particles, remains at high temperature for a long time. On the downstream side, the reattachment of the flow farther away, could lead to multiple, complex interactions with successive buildings, rendering the impact of a PDC quite inhomogeneous over inhabited areas. The burning, as well as the upper flow buoyancy over the building (Eq. (9) in Supplementary material), would be further enhanced at temperatures higher than that used in our simulation (573 K). The horizontal component of dynamic pressure is important for addressing the impact of PDCs over buildings, as acknowledged in other volcanological studies in which the resistance of walls, doors and windows is considered (Baxter et al., 2005; Valentine, 1998). However, the strong upward component of dynamic pressure, resulting from flow–building interaction, can also severely affect structural elements, such as roofs and balconies, extending out from the building, which can be dramatically exposed to the effect of the current. This work represents the first attempt of quantifying directly the interaction between a PDC and a building, and is consistent with the findings of Gurioli et al. (2002, 2005) that investigated in the field the effect of the PDC of Pompeii and Herculaneum in the area of Vesuvius. Finally, we suggest that, for a careful investigation of the hazardous effects of PDCs, the flow–multibuilding interaction needs to be considered by 3D simulation over the real landscape of the inhabited areas around active volcanoes, and compared with results of experiments with multiple mock-ups, which will be done in the future to better understand the interaction between a PDC and a city.

Supplementary materials related to this article can be found online at doi:10.1016/j.epsl.2011.08.017.

Acknowledgments

Michael Ort and James White greatly helped improving the manuscript.

References

Anderson, J.D., 1995. Computational Fluid Dynamics. McGraw-Hill.
Bakker, A., 2008. Extensive multiphase flow capabilities. Ansys Advant. 2 (4), 43–45.
Balachandar, S., Eaton, J.K., 2010. Turbulent dispersed multiphase flow. Ann. Rev. Fluid Mech. 42, 111–133.
Baxter, P.J., Boyle, R., Cole, P., Neri, A., Spence, R.S., Zuccaro, G., 2005. The impacts of pyroclastic surges on buildings at the eruption of the Soufrière Hills volcano. Montserrat. Bull. Volcanol. 67, 292–313.
Blocken, B., Carmeliet, J., 2006. The influence of the wind-blocking effect by a building on its wind-driven rain exposure. J. Wind. Eng. Ind. Aerodyn. 94, 101–127.
Blocken, B., Carmeliet, J., 2007. Validation of CFD simulations of wind-driven rain on a low-rise building facade. Build. Environ. 42 (7), 2530–2548.
Branney, M.J., Kokelaar, P., 2002. Pyroclastic density currents and the sedimentation of ignimbrites. Geological Society, Memoirs 27 London.
Cantero, M.I., Garcia, M.H., Balachandar, S., 2008. Effect of particle inertia on the dynamics of depositional particulate density currents. Comput. Geosci. 34, 1307–1318.
Cas, R.A.F., Wright, J.V., 1987. Volcanic Successions: Modern and Ancient. Allen & Unwin, London.
Cebeci, T., Cousteix, J., 1999. Modeling and Computation of Boundary Layer Flows. Springer, New York.
Crowe, C.T., 2000. On models for turbulence modulation in fluid–particle flows. Int. J. Multiphase Flow 26, 719–727.
Crowe, C.T., 2006. Multiphase Flow Handbook. Taylor & Francis Group, LLC.
Dartevelle, S., Rose, W.I., Stix, J., Kelfoun, K., Wallance, J.W., 2004. Numerical modeling of geophysical granular flows: 2. Computer simulation of Plinian clouds and pyroclastic flows and surges. Geochem. Geophys. Geosyst. 5, Q08004.
Defraeye, T., Blocken, B., Carmeliet, J., 2010. CFD analysis of convective heat transfer at the surfaces of a cube immersed in a turbulent boundary layer. Int. J. Heat Mass Transfer 53, 297–308.
Dellino, P., Mele, D., Bonasia, R., Braia, G., La Volpe, L., Sulpizio, R., 2005. The analysis of the influence of pumice shape on its terminal velocity. Geophys. Res. Lett. 32 (L2), L21306.
Dellino, P., Zimanowski, B., Buttner, R., La Volpe, L., Mele, D., Sulpizio, R., 2007. Large-scale experiments on the mechanics of pyroclastic flow: design, engineering, and first results. J. Geophys. Res. 112, B04202.
Dellino, P., Mele, D., Sulpizio, R., La Volpe, L., Braia, G., 2008. A method for the calculation of the impact parameters of dilute pyroclastic density currents based on deposits particle characteristics. J. Geophys. Res. 113, B07206.
Dellino, P., Dioguardi, F., Zimanowski, B., Buttner, R., Mele, D., La Volpe, L., Sulpizio, R., Doronzo, D.M., Sonder, I., Bonasia, R., Calvari, S., Marotta, E., 2010a. Conduit flow experiments help constraining the regime of explosive eruptions. J. Geophys. Res. 115, B04204.
Dellino, P., Buttner, R., Dioguardi, F., Doronzo, D.M., La Volpe, L., Mele, D., Sonder, I., Sulpizio, R., Zimanowski, B., 2010b. Experimental evidence links volcanic particle characteristics to pyroclastic flow hazard. Earth Planet. Sci. Lett. 295, 314–320.
Doronzo, D.M., 2010. Could the Twin Towers collapse teach the interaction between dilute pyroclastic density currents and buildings? Nat. Hazard. 55, 177–179.
Doronzo, D.M., Dellino, P., 2010. A fluid dynamic model of volcaniclastic turbidity currents based on the similarity with the lower part of dilute pyroclastic density currents: Evaluation of the ash dispersal from ash turbidites. J. Volcanol. Geotherm. Res. 191, 193–204.
Doronzo, D.M., Valentine, G.A., Dellino, P., de Tullio, M.D., 2010. Numerical analysis of the effect of topography on deposition from dilute pyroclastic density currents. Earth Planet. Sci. Lett. 300, 164–173.
Doronzo, D.M., de Tullio, M.D., Dellino, P., Pascazio, G., 2011. Numerical simulation of pyroclastic density currents using locally refined Cartesian grids. Comput. Fluids 44, 56–67.
Dufek, J., Bergantz, G.W., 2007. Suspended-load and bed-load transport of particle-laden gravity currents: the role of particle–bed interaction. Theor. Comput. Fluid Dyn. 21, 119–145.
Esposti Ongaro, T., Clarke, A., Neri, A., Voight, B., Widiwijayanti, C., 2008. Fluid-dynamics of the 1997 Boxing Day lateral blast of Soufrière Hills volcano (Montserrat, WI). J. Geophys. Res. 113, B03211.
Ferziger, J.H., Peric, M., 2002. Computational Method for Fluid Dynamics. Springer.
Fletcher, C.A.J., 1991. Computational Techniques for Fluid Dynamics, vol. 1 and 2. Springer.
Fluent 6.3, 2006. Manual 2006. Fluent Inc.
Furbish, D.J., 1997. Fluid Physics in Geology. Oxford University Press, New York.
Giordano, G., 1998. The effect of paleotopography on lithic distribution and facies associations of small volume ignimbrites: the WTT Cupa (Roccamonfina volcano, Italy). J. Volcanol. Geotherm. Res. 87, 255–273.
Gurioli, L., Cioni, R., Sbrana, A., Zanella, E., 2002. Transport and deposition of pyroclastic density currents over an inhabited area: the deposits of the AD 79 eruption of Vesuvius at Herculaneum, Italy. Sedimentol. 49, 1–26.
Gurioli, L., Pareschi, M.T., Zanella, E., Lanza, R., Deluca, E., Bisson, M., 2005. Interaction of pyroclastic density currents with human settlements: evidence from ancient Pompeii. Geology 33, 441–444.
Hallworth, M.A., Phillips, J.C., Huppert, H.E., Sparks, R.S.J., 1993. Entrainment in turbulent gravity currents. Nature 362, 829–831.
Hoffmann, P.H., Muck, K.C., Bradshaw, P., 1985. The effect of concave surface curvature on turbulent boundary layers. J. Fluid Mech. 161, 371–403.
Middleton, G.V., Southard, J.B., 1984. Mechanics of Sediment Movement. Soc. Econ. Paleont. Mineral, Tulsa, OK.
Muck, K.C., Hoffmann, P.H., Bradshaw, P., 1985. The effect of convex surface curvature on turbulent boundary layers. J. Fluid Mech. 161, 347–369.

Neri, A., Esposti Ongaro, T., Macedonio, G., Gidaspow, D., 2003. Multiparticle simulation of collapsing volcanic columns and pyroclastic flow. J. Geophys. Res. 108 (B4), 2202.
Patankar, S.V., 1980. Numerical Heat Transfer and Fluid Flow. Hemisphere, New York.
Pope, S.B., 2000. Turbulent Flows. Cambridge University Press.
Raga, A.C., Cantó, J., 2008. Turbulent entrainment in Mira's cometary tail. Astrophys. J. 685, L141.
Rouse, H., 1939. An analysis of sediment transportation in the light of fluid turbulence. Soil Conservation Services Report No.SCS-TP-25, USDA, Washington, D.C.
Schlichting, H., Gersten, K., 2000. Boundary Layer Theory. Springer.
Shih, T.H., Liou, W.W., Shabbir, A., Zang, Z., Zhu, J., 1995. A new k–ε eddy-viscosity model for high Reynolds number turbulent flows: model development and validation. Comput. Fluids 24 (3), 227–238.
Sulpizio, R., Mele, D., Dellino, P., La Volpe, L., 2005. A complex, Subplinian-type eruption from low-viscosity, phonolitic to tephri-phonolitic magma: the AD 472 (Pollena) eruption of Somma-Vesuvius (Italy). Bull. Volcanol. 67, 743–767.
Valentine, G.A., 1987. Stratified flow in pyroclastic surges. Bull. Volcanol. 49, 616–630.
Valentine, G.A., 1998. Damage to structures by pyroclastic flows and surges, inferred from nuclear weapons effects. J. Volcanol. Geotherm. Res. 87, 117–140.
Valentine, G.A., Wohletz, K.H., 1989. Numerical models of Plinian eruptions columns and pyroclastic flows. J. Geophys. Res. 94, 1867–1887.
Valentine, G.A., Doronzo, D.M., Dellino, P., de Tullio, M.D., 2011. Effects of volcano profile on dilute pyroclastic density currents: numerical simulations. Geology 39, 947–950.
Versteeg, H.K., Malalasekera, W., 2007. An Introduction to Computational Fluid Dynamics: The Finite Volume Method. Prentice Hall.